

# On the discrepancies between theoretical and measured below-cloud particle scavenging coefficients for rain – a numerical investigation using a detailed one-dimensional cloud microphysics model

X. Wang<sup>1</sup>, L. Zhang<sup>2</sup>, and M. D. Moran<sup>2</sup>

<sup>1</sup>Kellys Environmental Services, Toronto, Canada

<sup>2</sup>Air Quality Research Division, Science and Technology Branch, Environment Canada, 4905 Dufferin Street, Toronto, Ontario, M3H 5T4, Canada

Received: 7 June 2011 – Published in Atmos. Chem. Phys. Discuss.: 18 July 2011

Revised: 4 November 2011 – Accepted: 14 November 2011 – Published: 29 November 2011

**Abstract.** Existing theoretical formulations for the size-resolved scavenging coefficient  $\Lambda(d)$  for atmospheric aerosol particles scavenged by rain predict values lower by one to two orders of magnitude than those estimated from field measurements of particle-concentration changes for particles smaller than  $3\ \mu\text{m}$  in diameter. Vertical turbulence is not accounted for in the theoretical formulations of  $\Lambda(d)$  but does contribute to the field-derived estimates of  $\Lambda(d)$  due to its influence on the overall concentration changes of aerosol particles in the layers undergoing impaction scavenging. A detailed one-dimensional cloud microphysics model has been used to simulate rain production and below-cloud particle scavenging, and to quantify the contribution of turbulent diffusion to the overall  $\Lambda(d)$  values calculated from particle concentration changes. The relative contribution of vertical diffusion to below-cloud scavenging is found to be largest for submicron particles under weak precipitation conditions. The discrepancies between theoretical and field-derived  $\Lambda(d)$  values can largely be explained by the contribution of vertical diffusion to below-cloud particle scavenging for all particles larger than  $0.01\ \mu\text{m}$  in diameter for which field data are available. The results presented here suggest that the current theoretical framework for  $\Lambda(d)$  can provide a reasonable approximation of below-cloud aerosol particle scavenging by rain in size-resolved aerosol transport models if vertical diffusion is also considered by the models.

## 1 Introduction

Precipitation scavenging is a major removal process for below-cloud aerosol particles. Due to the complex interactions between particles and raindrops, the scavenging process needs to be parameterized in the mass continuity equations used in atmospheric chemical transport models (CTMs). The parameter known as scavenging coefficient ( $\Lambda$ ), which is defined as the time rate of change of the ambient concentration of aerosol particles due to precipitation scavenging, is often used to quantify this process (e.g. Seinfeld and Pandis, 2006). Different formulations of  $\Lambda$  apply to bulk particle number, bulk particle mass, and size-resolved particle number or mass concentrations (e.g. Zhang et al., 2004). Theoretical size-resolved formulas for  $\Lambda$  are typically parameterized as a function of collection efficiency, in which some or most of the known particle-droplet collection mechanisms, including Brownian diffusion, interception, impaction, thermo- and diffusiophoresis, and electrostatic forces, are considered (e.g. Slinn, 1983; Andronache et al., 2006; Loosmore and Cederwall, 2004; Chate et al., 2003; Chate, 2005; Chate and Pranesha, 2004; Park et al., 2005; Henzing et al., 2006; Tost et al., 2006; Feng, 2007; Croft et al., 2009).

It has long been known, however, that size-resolved values of  $\Lambda(d)$  calculated from all existing theoretical parameterizations are one to two orders of magnitude smaller than the majority of field measurements of  $\Lambda(d)$  for all particle sizes except those larger than  $3\ \mu\text{m}$  in diameter  $d$ , for which theoretical and field  $\Lambda(d)$  values agree well. Turbulence is suspected to play a key role in these large discrepancies as supported by limited measurements collected under controlled conditions (Sparmacher et al., 1993). Turbulence may increase droplet/aerosol collision efficiency due



Correspondence to: L. Zhang  
(leiming.zhang@ec.gc.ca)

to turbulent flow fluctuations (Grover and Pruppacher, 1985; Khain and Pinsky, 1997). Turbulent diffusion in the atmospheric boundary layer may increase the mixing of particle and droplet populations and thus increase their collision frequencies. Turbulent diffusion may also transport aerosol particles from the subcloud layer into the cloud layer followed by in-cloud scavenging (Andronache et al., 2006).

In the present study we have employed a detailed one-dimensional aerosol-cloud microphysics numerical model to investigate the contribution of vertical turbulent diffusion to overall below-cloud aerosol particle scavenging. If this contribution could be quantified, we would have a better idea of whether or not there is a need to modify existing theoretical  $\Lambda(d)$  formulations. CARMA (Community Aerosol and Radiation Model for Atmospheres), the detailed aerosol-cloud microphysics model that has been used in this study, was originally developed at the NASA Ames Research Center (Toon et al., 1988; Ackerman et al., 1995) and was later modified by Zhang et al. (2004) to produce light precipitation from low-level warm stratiform clouds in order to study below-cloud precipitation scavenging by rain. A similar approach is used here to produce rain with intensities from 0.1 to 5 mm h<sup>-1</sup> for studying below-cloud aerosol particle scavenging (i.e. “wash-out”) under conditions with and without the presence of vertical turbulent diffusion. The numerical simulation results provide some guidance on the source of the differences between theoretical formulations and field measurements of  $\Lambda(d)$  and on future research needs.

## 2 Methodology

### 2.1 Model formulation

A brief description of the theoretical basis for and the algorithms used in CARMA is provided below; additional details may be found in Toon et al. (1988) and Ackerman et al. (1995). Conceptually, two distinct particle populations are considered in this cloud microphysics model, one corresponding to unactivated aerosol particles and the other to liquid droplets, including both cloud droplets and raindrops. One-dimensional continuity equations of identical form apply to the two particle populations:

$$\frac{\partial C}{\partial t} = \frac{C}{\rho} \frac{\partial \rho w}{\partial z} - \frac{\partial}{\partial z} [(w - V_f)C] + \frac{\partial}{\partial z} [K_z \rho \frac{\partial (C/\rho)}{\partial z}] + P - L \quad (1)$$

where  $C(d, z, t)$  (m<sup>-3</sup> μm<sup>-1</sup>) is the number concentration of either particle population for a size bin and is a function of particle diameter  $d$  (μm), vertical height  $z$  (m), and time  $t$  (s);  $C(d, z, t)dd$  represents the mean number concentration (m<sup>-3</sup>) of particles or droplets having diameter between  $d$  and  $d+dd$ ;  $\rho(z, t)$  is the density of dry air (kg m<sup>-3</sup>);  $w(z, t)$  is the vertical air velocity (m s<sup>-1</sup>);  $V_f(d, z)$  is the particle settling velocity (m s<sup>-1</sup>) for each of the particle populations;  $K_z(z)$  is the vertical diffusion coefficient (m<sup>2</sup> s<sup>-1</sup>); and  $P$  and  $L$

represent production and loss terms, respectively, of particles or droplets due to microphysical processes.

The first term on the right side of Eq. (1) represents the horizontal divergence that compensates for any changes in air density due to vertical convergence. The second term represents the divergence of the vertical flux due to vertical advection and sedimentation. The third term represents the divergence of the vertical flux due to turbulent diffusion. Lastly, the production and loss terms include the following processes: (i) activation of aerosol particles (i.e. cloud nuclei) into cloud droplets; (ii) condensation/evaporation of droplets; and (iii) collision-coalescence of particle pairs (self-coagulation), droplet pairs, and particle-droplet pairs (collection). Note that aerosol activation is a loss process for particles but a production process for droplets; full evaporation of droplets is a loss process but a production process for particles; and collision-coalescence is a loss process for particles only, droplets only, or both particles and droplets. The two continuity equations are thus coupled via the  $P$  and  $L$  terms. As well, the theoretical formulation of the scavenging coefficient represents the aggregate impact of the  $P$  and  $L$  terms mentioned above.

The treatment for the collection processes for particle-droplet pairs in CARMA takes into account the contributions from Brownian motion, convective Brownian diffusion enhancement, and the gravitational collection of particles by droplets because of differences in their fall speeds. The algorithms for the first two collection processes follow the formulas given by Jacobson (2005). The gravitational collection efficiency is treated as the product of collision efficiency and coalescence efficiency. The collision efficiencies are interpolated from a look-up table given by Vohl et al. (2007) which was derived from laboratory experiments. The table provides collision efficiency values for a wider range of collector particle sizes (i.e. from 20 to 1200 μm in diameter) than previous existing tables (e.g. Hall, 1980). The formulation of Beard and Ochs (1984) is employed for coalescence efficiency.

Note that one limitation of even the detailed microphysical formulation used by CARMA for testing the impact of flow turbulence on collection efficiency is that vertical turbulent diffusion is treated as a separate process from the particle-droplet collision-coalescence process. Thus, enhancement of collection efficiency by turbulence cannot be modeled directly, but the subgrid-scale mixing of both particle and droplet populations is accounted for, which has the effect of increasing collision frequencies through increased mixing and contact of the two populations.

### 2.2 Model configuration

The vertical domain of the model is specified to go from the surface to 6 km with 141 unevenly spaced vertical levels. For the vertical discretization, 10 m is chosen for the lowest of the 141 layers, gradually increasing to 40 m at 400 m, and then held at 40 m up to the model top. A vertical velocity

profile is prescribed, with peak values at the initial cloud mid-height at 2250 m and decreasing to zero at both the initial cloud base (1000 m) and cloud top (3500 m), to form the cloud layer and subsequent precipitation. The peak vertical wind of  $0.15 \text{ m s}^{-1}$  is used to drive the model to generate weak and moderate precipitation and  $0.45 \text{ m s}^{-1}$  is used to generate strong precipitation. These values are based on field measurements as referenced in Zhang et al. (2004). For example, Yum and Hudson (2001) pointed out that the mean vertical velocity inside stratiform clouds is usually less than  $0.5 \text{ m s}^{-1}$  while peak values can be larger than  $2 \text{ m s}^{-1}$ . For convective clouds, the vertical wind velocity in cloud can be of the order of  $1.0 \text{ m s}^{-1}$  or more (e.g. Nuber and Graf, 2005).

The vertical diffusion coefficient  $K_z$  is parameterized according to Brost and Wyngaard (1978):

$$K_z = \kappa u_* z \left(1 - \frac{z}{h}\right)^{1.5} \left(1 - B \frac{d\theta}{dz}\right), \quad (2)$$

where  $\kappa$  is the von Kármán constant ( $\approx 0.4$ ),  $u_*$  is the friction velocity,  $h$  is the boundary-layer height,  $B$  is an empirical constant, taken to be  $40 \text{ m K}^{-1}$ , and  $\theta$  is potential temperature.

Two sets of 50 size bins are used to represent the aerosol particle and droplet size distributions in the integration of Eq. (1). The bin diameters ranged from  $0.001$  to  $100 \mu\text{m}$  for aerosol particles and from  $1 \mu\text{m}$  to  $10 \text{ mm}$  for droplets; constant volume ratios of 2.12 and 1.78, respectively, are specified between successive bins. Since cloud droplets as small as a few microns and raindrops as large as a few millimeters in diameter are considered in this cloud microphysics model, it is necessary to use a large number of size bins to cover this large range of hydrometeor sizes. Note, however, that this does not mean that small droplets can reach the Earth's surface, given their very small fall velocities and the upward grid-scale vertical velocity that has been prescribed. Thus, concentrations of small droplets are not significantly different from zero at below-cloud levels.

The initial three-mode, rural-type size distribution of the aerosol particles, their chemical composition and vertical distribution, and the initial conditions of vertical profiles of temperature and relative humidity that are specified, follows Zhang et al. (2004). CARMA has then been integrated forward in time in each simulation with this configuration and a time step of 10 s.

### 2.3 Sensitivity test design

By specifying different peak vertical velocities at the center of the designed cloud layer, with cloud base at 1000 m and cloud top at 3500 m, different precipitation intensities near the surface can be obtained at different integration times. Three precipitation intensities, representing weak ( $0.1 \text{ mm h}^{-1}$ ), moderate ( $1 \text{ mm h}^{-1}$ ), and strong ( $5 \text{ mm h}^{-1}$ ) precipitation, respectively, are chosen for the present study. For each of these three precipitation intensities, four sensitivity tests have been conducted using different vertical profiles

of the vertical diffusion coefficient  $K_z$  for a total of 12 simulations. Test 1 represents the situation with no vertical diffusion ( $K_z = 0$ ), while Tests 2 to 4 correspond to extremely weak, relatively weak, and strong vertical diffusion conditions, respectively (see Fig. 1 for the  $K_z$  profiles used for Tests 2 to 4).

Once the precipitation intensity at near-surface levels reaches one of the three specific values designed for our sensitivity tests (i.e.  $0.1$ ,  $1$ , and  $5 \text{ mm h}^{-1}$ ), the below-cloud particle number concentration profile is restored to its initial profile for the purpose of tracking concentration changes in order to calculate the size-resolved scavenging coefficient  $\Lambda(d)$  using the formula (e.g. Seinfeld and Pandis, 2006)

$$\Lambda(d) = -\frac{1}{\Delta t} \frac{C(d, t_2) - C(d, t_1)}{C(d, t_1)}, \quad (3)$$

where  $C(d, t_1)$  and  $C(d, t_2)$  are particle number concentrations at the beginning and end, respectively, of a time period  $\Delta t$ . Note that while meteorological variables are assigned at grid levels, concentrations are assigned at grid half-levels. Also, to avoid any artificial effect of the lower boundary conditions, model results from the second-lowest model half-level ( $16 \text{ m}$  mid-layer height as marked in Fig. 1) are used for the  $\Lambda(d)$  calculation.

The 12 model runs described above are conducted for relatively short time periods in order to keep the precipitation intensities close to the design values (see also next section). Results from these 12 runs are shown in Fig. 2 and Table 1. An additional set of model runs (with no fixed precipitation intensity but aiming for weak precipitation) is also conducted for a much longer period to confirm the results from the first 12 runs (see Sect. 3.2).

## 2.4 Methodological factors to consider

### 2.4.1 Choice of time interval $\Delta t$ to estimate $\Lambda(d)$

Due to the change of model-predicted precipitation intensity with time, the  $\Delta t$  value chosen for Eq. (3) cannot be too large if we want to compare model-based  $\Lambda(d)$  values conducted under specific precipitation rate conditions ( $0.1$ ,  $1.0$ , and  $5.0 \text{ mm h}^{-1}$ ) with field measurements. For the first two cases ( $0.1$  and  $1.0 \text{ mm h}^{-1}$ ), the modeled precipitation rate maintains a relatively constant value for a period of 20 min whereas for the third case, the precipitation rate only stays close to  $5.0 \text{ mm h}^{-1}$  for  $\sim 6$  min. Thus,  $\Delta t$  values of 20, 20, and 6 min are chosen for  $\Lambda(d)$  calculations using Eq. (3) (see Table 1). Using a value of 20 min for  $\Delta t$  is also reasonable considering that the major applications of the theoretical "scavenging coefficient" formulas are to numerical air-quality models and the time step in these models is typically on the order of 20 min.

It should be noted that in the real world it takes hours under weak precipitation conditions for scavenging to remove a detectable amount of submicron particles. Thus, in field experiments, the time period considered for measuring particle

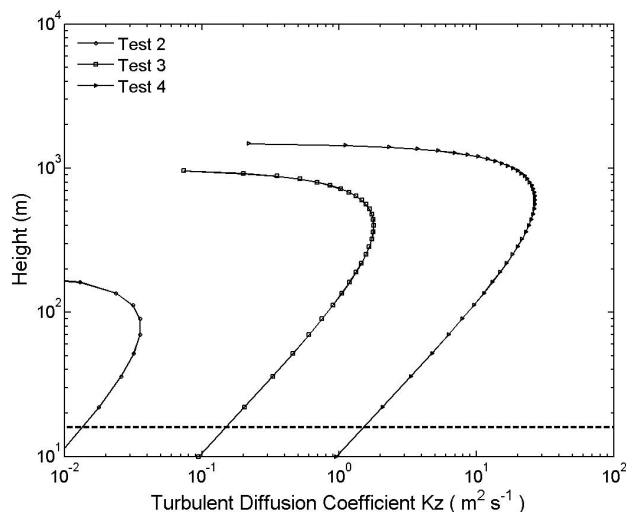


**Fig. 1.** Vertical profiles of the vertical diffusion coefficient  $K_z$  used for the sensitivity tests in which the boundary-layer height was chosen to be 200, 1000, and 1500 m, respectively. The horizontal dashed line marks the 16-m model half level.

concentrations (before, during, and after rain events) has to be more than a few hours in order to generate any meaningful scavenging coefficient values; e.g. the amount scavenged has to be larger than the instrument detection limit and the measurement uncertainties. These concerns will not be an issue in numerical model studies, so we have the liberty to choose a much smaller  $\Delta t$  value. It should be further noted that  $\Lambda(d)$  calculated from Eq. (3) for slow-scavenged (e.g. submicron) particles will not differ significantly when using different  $\Delta t$  values (e.g. from 20 min to 6 h). However, the use of a too large  $\Delta t$  value in Eq. (3) will cause  $\Lambda(d)$  to be underestimated for fast-scavenged (e.g. supermicron) particles due to the exponential decay of particle concentrations during the precipitation scavenging process.

#### 2.4.2 Processes contributing to $\Lambda(d)$ estimates

The scavenging coefficient  $\Lambda(d)$  calculated from the theoretical formulations only accounts for the process of droplet-particle collection whereas  $\Lambda(d)$  calculated from Eq. (3) accounts for the concentration changes predicted by the full Eq. (1) and may include contributions from all of the processes considered, including turbulent diffusion, advection, sedimentation, and all of the microphysical production and loss processes. These processes are the main factors determining the fate of atmospheric aerosols during precipitation (Laakso et al., 2003).

Horizontal advection may affect field measurements of aerosol concentration if the background air mass changes between measurements due to relatively long sampling periods. However, such air-mass changes can easily be recognized based on analysis of related meteorological parameters such

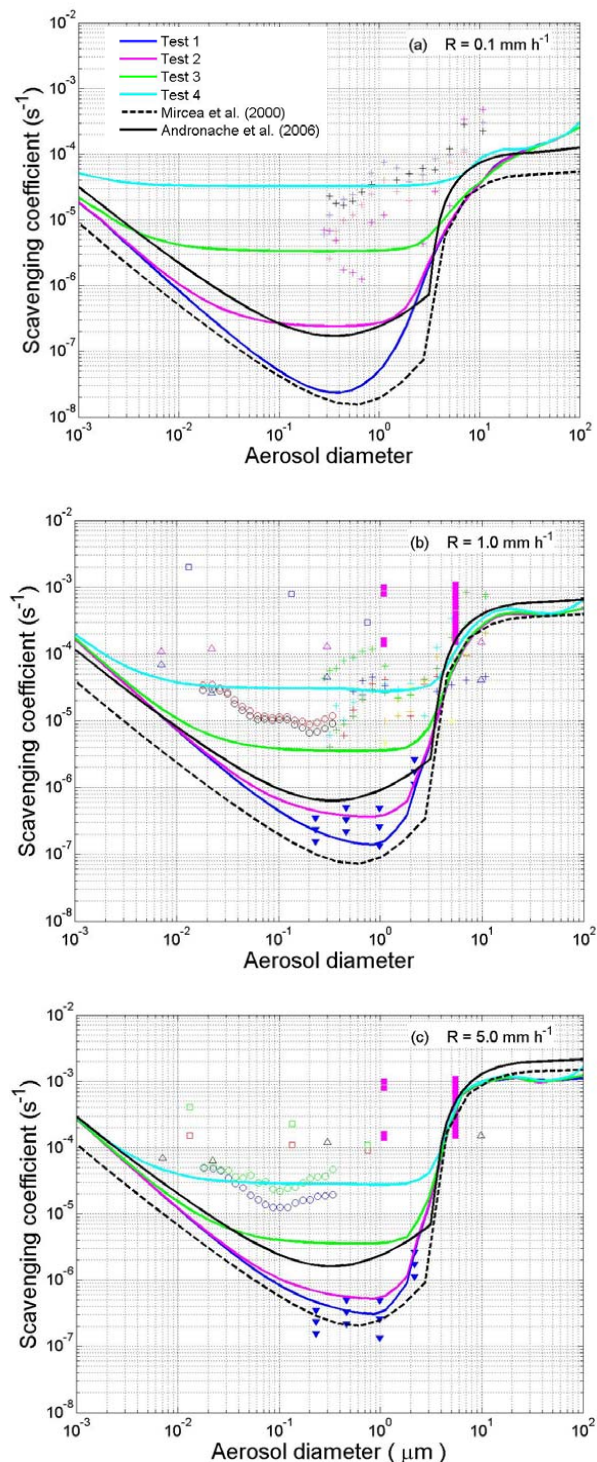


**Fig. 2.** Size-resolved scavenging coefficient  $\Lambda(d)$  for three precipitation intensities  $R$  calculated from model-predicted concentration changes at 16 m height for tests with and without vertical turbulent diffusion (four solid colored lines). Also shown are scavenging coefficients from two theoretical parameterizations (two black lines) representing the range of existing theoretical formulations. Available measurements of  $\Lambda(d)$  are copied from Wang et al. (2010) and are shown by various symbols.

**Table 1.** Percentage removal ( $\eta(d) = -\Delta C(d)/C(d) \times 100\%$ ) and the corresponding scavenging coefficient  $\Lambda(d)$  ( $\times 10^{-5} \text{ s}^{-1}$ ) at 16 m predicted from Eq. (3) for five selected particle sizes ( $d = 0.005, 0.05, 0.5, 2.0$  and  $5.0 \mu\text{m}$ ) from the four  $K_z$  sensitivity tests ( $K_z = 0, 0.013, 0.15$  and  $1.5 \text{ m}^2 \text{ s}^{-1}$  at 16 m) under three precipitation intensities ( $\bar{R} = 0.1, 1.0$  and  $5.0 \text{ mm h}^{-1}$ ).

$K_z$ Sensitivity Tests		Test 1					Test 2					Test 3					Test 4				
Particle diameter ( $d, \mu\text{m}$ )		0.005	0.05	0.5	2.0	5.0	0.005	0.05	0.5	2.0	5.0	0.005	0.05	0.5	2.0	5.0	0.005	0.05	0.5	2.0	5.0
$\bar{R} = 0.1 \text{ mm h}^{-1}$ $\Delta t = 1200 \text{ s}$ $P = 0.033 \text{ mm}$	$\eta(d)$	0.18	0.01	0.01	0.10	0.91	0.22	0.04	0.04	0.14	0.98	0.60	0.42	0.42	0.57	1.61	4.19	4.02	4.02	4.20	4.82
	$\Lambda(d)$	0.15	0.01	0.01	0.08	0.76	0.18	0.04	0.03	0.12	0.82	0.50	0.35	0.35	0.48	1.35	3.50	3.35	3.35	3.50	4.02
$\bar{R} = 1.0 \text{ mm h}^{-1}$ $\Delta t = 1200 \text{ s}$ $P = 0.33 \text{ mm}$	$\eta(d)$	1.79	0.10	0.02	0.22	5.49	1.82	0.13	0.06	0.27	5.57	2.22	0.52	0.44	0.71	5.40	5.54	3.82	3.70	3.74	6.19
	$\Lambda(d)$	1.49	0.08	0.02	0.18	4.58	1.52	0.11	0.05	0.22	4.64	1.85	0.43	0.37	0.59	4.50	4.62	3.19	3.08	3.12	5.16
$\bar{R} = 5.0 \text{ mm h}^{-1}$ $\Delta t = 360 \text{ s}$ $P = 0.5 \text{ mm}$	$\eta(d)$	0.88	0.05	0.01	0.17	9.07	0.89	0.06	0.02	0.19	9.05	1.01	0.17	0.13	0.32	9.32	1.88	1.09	1.04	1.20	10.0
	$\Lambda(d)$	2.45	0.15	0.04	0.47	25.2	2.48	0.18	0.07	0.51	25.1	2.79	0.48	0.37	0.90	25.89	5.22	3.02	2.90	3.32	27.77

$\bar{R}$ : average precipitation intensity ( $\text{mm h}^{-1}$ ) during the time period  $\Delta t$ .

$\Delta t$ : time interval selected to calculate the mean model-derived  $\Lambda(d)$  values based on Eq. (3).

$P$ : total amount of rain (mm) during the time period  $\Delta t$ .

as temperature, humidity, wind speed and direction, etc., and can therefore be excluded when calculating  $\Lambda(d)$  values (Volken and Schumann, 1993; Laakso et al., 2003). Therefore, horizontal advection should not be the main source of the large discrepancies between theoretical and field-derived  $\Lambda(d)$  values. In the present one-dimensional model simulation, horizontal-advection effects are also excluded.

Sensitivity tests on sedimentation showed that the impact of this process on  $\Lambda(d)$  estimates is more than two orders of magnitude smaller than that from the collection process for particles smaller than  $3 \mu\text{m}$  in diameter and the effect is only noticeable for particles larger than  $5 \mu\text{m}$  in diameter under weak precipitation and for particles larger than  $10 \mu\text{m}$  under moderate to strong precipitation. Thus, this process is also not a factor in the discrepancy of  $\Lambda(d)$  between theoretical results and field-derived values. It should be noted, however, that sedimentation (and dry deposition) can be as or more important than precipitation scavenging on a monthly or annual basis.

It has been shown by both theoretical and field studies that droplet evaporation process may affect aerosol scavenging due to the creation of new particles. For example, numerical studies in Zhang et al. (2004) that used the same cloud microphysics model as the one used here sometimes produced negative scavenging coefficient estimates for submicron particles (new particles evaporated from raindrops are distributed as a log-normal distribution to avoid accumulation into one size bin). A recent field study conducted by Defence Research and Development Canada Suffield (J. Ho, personal communication, 2011) also showed negative scavenging coefficients for submicron particles. Theoretically, evaporation should have the largest impact when precipitation first begins and the sub-cloud layer is the driest. When relative hu-

midity (RH) approaches 100% near the surface due to continued moistening from raindrop evaporation, the effects of evaporation on aerosol concentration should then be small. This reasoning has also been confirmed by our numerical sensitivity tests. In the present study, we first let precipitation develop and fall to the surface for some time so that the precipitation intensity reaches a preferred value and the surface RH reaches a value close to 100%. We then introduce a prescribed vertical profile of size-distributed aerosol particles into the model in order to investigate the below-cloud particle scavenging. Thus, the impact of raindrop evaporation on the calculated  $\Lambda(d)$  in our sensitivity tests has been minimized.

The activation of aerosol particles to form droplets only occurs under supersaturated conditions inside clouds and should not be a concern near the surface (fog is an exception but is not relevant to the cases studied here). Sensitivity tests on self-coagulation of aerosol particles (by turning the process on and off in the model) shows negligible impacts from this process compared to droplet-aerosol particle coagulation and thus negligible impact to modeled  $\Lambda(d)$  values.

Based on the above considerations, the key processes that affect the model-derived  $\Lambda(d)$  values should be droplet-particle collection processes and turbulence diffusion. It should be noted that since  $K_z$  is set to zero (no vertical diffusion) in Test 1, contributions from any of the processes discussed above, if non-negligible, would be included in the  $\Lambda(d)$  values estimated in Test 1. Any differences between Test 1 and the other tests (Tests 2–4) should thus be attributable to the vertical diffusion process.

### 3 Results

#### 3.1 The effect of turbulent diffusion on $\Lambda(d)$

The modeled  $\Lambda(d)$  distributions for the three different precipitation intensities with four different  $K_z$  profiles (a total of 12 model runs) are shown in Fig. 2 (see four colored solid lines in each panel). Concentration changes (in terms of percentage, hereafter referred to  $\eta(d)$ ) and the corresponding  $\Lambda(d)$  values for five selected particle sizes are presented in Table 1 for these 12 model runs. Also shown in Fig. 2 are  $\Lambda(d)$  distributions from two theoretical formulations, Mircea et al. (2000) (black dashed line) and Andronache et al. (2006) (black solid line), which represent the range of existing theoretical formulations (see Wang et al., 2010). Both of these parameterizations were developed based on the concept of collection efficiency discussed by Slinn (1983). The parameterization of Mircea et al. (2000) takes into account the three most important collection mechanisms for below-cloud particle scavenging (Brownian diffusion, interception, and inertial impaction) while that of Andronache et al. (2006) considers several additional collection mechanisms due to thermophoresis, diffusiphoresis, and electrostatic forces.

With the vertical diffusion coefficient set to 0 in Test 1,  $\Lambda(d)$  calculated from modeled concentrations using Eq. (3) is mainly a result of particle-droplet collection (collision and coalescence) processes. Contributions from other processes are negligible as discussed in Sect. 2.4. As expected,  $\Lambda(d)$  calculated for Test 1 fall in between the two black lines representing the range of existing theoretical  $\Lambda(d)$  formulations for all particle sizes for the three precipitation intensities considered (Fig. 2). The differences between the  $\Lambda(d)$  distribution calculated for Test 1 and the two theoretical  $\Lambda(d)$  formulations are simply caused by differences in their treatments of collection efficiency, droplet spectrum, and to a less extent, terminal fall velocity, and these differences in  $\Lambda(d)$  are generally within one order of magnitude (Wang et al., 2010). As shown in Fig. 2, these theoretical  $\Lambda(d)$  distributions (including Test 1 here) are also of the same order of magnitude as those calculated for one controlled experiment of Sparmaier et al. (1993), for which turbulence effects were minimized. However, they are almost two orders of magnitudes smaller than  $\Lambda(d)$  values derived from the majority of other field experiments.

In Test 1, large particles of diameter  $5\ \mu\text{m}$  are removed by 1 % and 5 %, respectively, under weak ( $\bar{R} = 0.1\ \text{mm h}^{-1}$ ) and moderate ( $\bar{R} = 1.0\ \text{mm h}^{-1}$ ) precipitation intensities in just 20 min, and by 9 % under strong precipitation intensity ( $\bar{R} = 5.0\ \text{mm h}^{-1}$ ) in just 6 min (Table 1). In comparison, very small particles of diameter  $0.005\ \mu\text{m}$  are removed by 0.2–2 %, particles of diameter  $2\ \mu\text{m}$  are removed by 0.1–0.2 %, and particles with diameters in the  $0.05\text{--}0.5\ \mu\text{m}$  range are removed by <0.1 % under the same precipitation conditions. While percentage concentration change  $\eta(d)$  increases substantially (by a factor of 2 to 10) from weak precipitation

intensity (with 0.033 mm total precipitation) to moderate precipitation intensity (with 0.33 mm total precipitation), it actually decreases from moderate precipitation intensity to strong precipitation intensity (with 0.5 mm total precipitation) for all particle sizes except particles of 5 diameter  $\mu\text{m}$ . Apparently, different droplet spectra associated with different precipitation intensities have caused these differences. These results suggest that the use of only precipitation amount is not sufficient to estimate the aerosol amount scavenged by different precipitation intensities correctly.

When the effect of vertical diffusion is considered in the model,  $\Lambda(d)$  values calculated using Eq. (3) increase as can be seen from the results for Tests 2–4 shown in Fig. 2 and in Table 1. For a very small but non-zero  $K_z$  value (Test 2:  $0.013\ \text{m}^2\ \text{s}^{-1}$  at 16 m height),  $\Lambda(d)$  only increases significantly for submicron particles and under weak precipitation conditions (Fig. 2a). When  $K_z$  is increased to  $0.15\ \text{m}^2\ \text{s}^{-1}$  at 16 m (Test 3),  $\Lambda(d)$  increases markedly relative to Test 2, i.e. by a factor of 5 to 10 for submicron particles under all precipitation conditions. However, the contribution of turbulent diffusion is negligible for very small (<0.01  $\mu\text{m}$  diameter) and very large (>3  $\mu\text{m}$ ) particles under moderate to strong precipitation conditions due to their already very high  $\Lambda(d)$  values (associated with Brownian diffusion and inertial impaction, respectively). These Test 3  $\Lambda(d)$  values are still smaller, however, than those from the majority of field measurements. Finally, when  $K_z$  is increased to a value representative of fully unstable turbulent conditions (Test 4:  $1.5\ \text{m}^2\ \text{s}^{-1}$  at 16 m), predicted  $\Lambda(d)$  values increase to a level comparable to the field measurements. It should be noted that under rainy conditions the turbulence intensity is generally strong, even at night. Thus, the  $K_z$  values considered in Test 4 are more representative of rainy conditions than those applied in Tests 1–3. These results suggest that most of the discrepancy between theoretical and field-derived  $\Lambda(d)$  distributions can be explained by the contribution of vertical turbulent diffusion, which is not considered in current theoretical  $\Lambda(d)$  formulations but which likely contributed to the  $\Lambda(d)$  values obtained in the field experiments.

It is also evident that the impact of vertical turbulent diffusion varies strongly with particle size. Comparing results for the fully-turbulent-diffusion (Test 4) and no-diffusion (Test 1) cases, for particles of diameter  $5\ \mu\text{m}$ ,  $\eta(d)$  increases by a factor of 5 (from 1 to 5 %) under weak precipitation condition but by much less under moderate and strong precipitation conditions (Table 1). In comparison,  $\eta(d)$  for particles of diameter  $0.005\ \mu\text{m}$  increases by a factor of 20 (from 0.2 % to 4 %) under weak precipitation conditions and by a factor of 2 to 3 under moderate and strong precipitation conditions (from 1.8 % to 5.5 % and from 0.9 % to 1.9 %, respectively). Most notably,  $\eta(d)$  for particles of diameter  $0.5\ \mu\text{m}$  increases by two to three orders of magnitude (from 0.01–0.04 % to a few percent) for all precipitation conditions. Overall, turbulent diffusion has the largest impact for submicron particles under weak precipitation conditions.

**Table 2.** Same as Table 1 but after 3 and 6 h of weak precipitation only.

$K_z$ Sensitivity Tests		Test 1					Test 2					Test 3					Test 4				
Particle diameter ( $d$ , $\mu\text{m}$ )		0.005 0.05 0.5 2.0 5.0					0.005 0.05 0.5 2.0 5.0					0.005 0.05 0.5 2.0 5.0					0.005 0.05 0.5 2.0 5.0				
$\bar{R} = 0.3 \text{ mm h}^{-1}$ $\Delta t = 3 \text{ h}$ $P = 0.91$	$\eta(d)$	16.84	0.95	0.18	0.11	1.95	16.82	1.22	0.50	1.22	2.70	17.60	1.94	1.22	5.66	17.28	64.28	25.23	17.76	41.15	51.10
	$\Lambda(d)$	1.56	0.09	0.02	0.01	0.18	1.56	0.11	0.05	0.11	0.25	1.63	0.18	0.11	0.52	1.60	5.95	2.34	1.64	3.81	4.73
$\bar{R} = 0.36 \text{ mm h}^{-1}$ $\Delta t = 6 \text{ h}$ $P = 2.15$	$\eta(d)$	39.65	2.56	0.43	0.44	14.66	39.45	3.03	1.07	3.12	19.68	52.36	4.41	12.79	32.76	76.07	87.79	35.02	24.20	76.12	81.78
	$\Lambda(d)$	1.84	0.12	0.02	0.02	0.68	1.83	0.14	0.05	0.14	0.91	2.42	0.20	0.59	1.52	3.52	4.06	1.62	1.12	3.52	3.79

### 3.2 Results from longer model runs

The results presented in Sect. 3.1 suggest that under fully turbulent conditions (Test 4) an appreciable fraction of particles of all sizes is removed in a short time interval (20 min and 6 min), whereas almost no submicron particles is removed in the same time interval under non-turbulent conditions (Test 1). As discussed in Sect. 2.4.1, it takes hours under weak precipitation conditions for a measurable fraction of submicron particles to be scavenged. To verify the conclusions reached in Sect. 3.1, an additional set of four simulations has been conducted with CARMA for weak precipitation conditions. Each simulation lasts more than 6 h and hence is more like a field experiment. The percentage concentration change  $\eta(d)$  and the corresponding  $\Lambda(d)$  calculated after 3 and 6 h of each of these simulations are shown in Table 2 for the same five selected particle sizes.

After three or six hours of weak precipitation, 0.1 to 40 % of particles of different sizes are scavenged under non-turbulence conditions while 18 to 88 % of particles are removed under fully turbulent conditions. The average precipitation intensity during the first 3 h is  $0.3 \text{ mm h}^{-1}$  and during all 6 h is  $0.36 \text{ mm h}^{-1}$ ; both values fall in between the cases of weak and moderate precipitation intensities shown in Table 1. Thus,  $\Lambda(d)$  values shown in Table 2 should be comparable to those  $\Lambda(d)$  values shown in Table 1 for weak and moderate precipitation conditions. This is indeed the case. For most particle sizes, no significance difference in calculated  $\Lambda(d)$  values is found between Tables 1 and 2, especially for particles in the 0.05 to  $2 \mu\text{m}$  diameter range. The differences for the smallest ( $0.005 \mu\text{m}$ ) and largest ( $5 \mu\text{m}$ ) particles can be explained by differences in precipitation intensity and averaging time as discussed in Sect. 2.4. Thus, the results from these longer simulations support the conclusions reached in Sect. 3.1 from shorter sampling.

## 4 Discussion and recommendations

Numerical sensitivity tests are designed for a detailed aerosol-cloud microphysics model to quantify the contribution of vertical turbulent diffusion to below-cloud particle scavenging by rain. Even weak turbulent diffusion can en-

hance  $\Lambda(d)$  significantly for submicron particles but has little impact on very small ( $<0.01 \mu\text{m}$ ) or very large ( $5.0 \mu\text{m}$ ) particles. Strong turbulent diffusion can increase  $\Lambda(d)$  by more than two orders of magnitude for submicron particles and by more than one order of magnitude for smaller particles. The contribution of turbulent diffusion to  $\Lambda(d)$  is also shown to vary inversely with precipitation intensity.

The results presented here suggest that vertical diffusion alone can explain almost all of the discrepancies between theoretical and field-derived  $\Lambda(d)$  for particles in the 0.01 to  $3 \mu\text{m}$  diameter range for which size-specific field data are available. This suggests in turn that existing theoretical formulations for  $\Lambda(d)$  can be applied without modification in those aerosol transport models in which a vertical diffusion term is already included in the mass continuity equation, although the recommendation in Wang et al. (2010) that the theoretical  $\Lambda(d)$  parameterization that predicts the highest scavenging coefficient values should be used still holds.

Although the present study quantifies the contributions of turbulent diffusion to the well-known discrepancies between theoretical and measured  $\Lambda(d)$ , other factors not considered here may also play a role. For example, flow fluctuations in the wake behind falling raindrops may enhance the collection of the aerosol particles to the rear of the drops. Electrostatic attraction may also enhance the collection of submicron particles in the wake region of the drop (Berg, 1970). The number of particles collected in the wake region of a drop may be larger by an order of magnitude or more than the number collected on the front side of the drop (Asset and Hutchins, 1967). Another earlier study reported collection efficiencies above unity and up to 2 and explained the large values of collision efficiency by a combination of wake effect and electrostatic charge effects, but the effects favor collection of very large particles (i.e. particles larger than  $26 \mu\text{m}$  in diameter) rather than submicron particles (Engelmann, 1965). Quantification of the wake effect requires further study.

It is also recommended that future field studies of precipitation scavenging should if possible be designed to include aerosol particles smaller than  $0.01 \mu\text{m}$  in diameter as well as other particle sizes. It is also recommended that field measurements be made simultaneously under both natural and controlled environmental conditions so that the effect

of vertical turbulent diffusion and many other processes can be separated from that of the particle-droplet collection process. For example, the scavenging coefficients can be extracted through the measurements of aerosol concentrations during rain events in both natural field environments and a controlled sampling volume in which near-surface turbulence is limited.

*Acknowledgements.* We greatly appreciate critical comments and valuable suggestions from two anonymous reviewers.

Edited by: H. Tost

## References

- Ackerman, A. S., Toon, O. B., and Hobbs P. V.: A model for particle microphysics, turbulent mixing, and radiative transfer in the stratocumulus-topped marine boundary layer and comparisons with measurements, *J. Atmos. Sci.*, 52, 1204–1236, 1995.
- Andronache, C., Grönholm, T., Laakso, L., Phillips, V., and Venäläinen, A.: Scavenging of ultrafine particles by rainfall at a boreal site: observations and model estimations, *Atmos. Chem. Phys.*, 6, 4739–4754, doi:10.5194/acp-6-4739-2006, 2006.
- Asset, G. and Hutchins, T. G.: Leeward deposition of particles on cylinders from moving aerosols, *Amer., Ind., Hyg., Ass., J.*, 348–353, 1967.
- Beard, K. V. and Ochs III, H. T.: Collection and coalescence efficiencies for accretion, *J. Geophys. Res.*, 89, 7165–7169, 1984.
- Berg, T. G. O.: Collection efficiency in washout by rain, *Precipitation Scavenging*, CONF 700601, US Atomic Energy Commission, 169–186, 1970.
- Brost, R. and Wyngaard, J. C.: A model study of the stably stratified planetary boundary layer, *J. Atmos. Sci.*, 35, 1427–1440, 1978.
- Chate, D. M.: Study of scavenging of submicron-sized aerosol particles by thunderstorm rain events, *Atmos. Environ.*, 39, 6608–6619, 2005.
- Chate, D. M. and Pranesha, T. S.: Field studies of scavenging of aerosols by rain events, *J. Aerosol Sci.*, 35, 695–706, 2004.
- Chate, D. M., Rao, P. S. P., Naik, M. S., Momin, G. A., Safai, P. D., and Ali, K.: Scavenging of aerosols and their chemical species by rain, *Atmos. Environ.*, 37, 2477–2484, 2003.
- Croft, B., Lohmann, U., Martin, R. V., Stier, P., Wurzler, S., Feichter, J., Posselt, R., and Ferrachat, S.: Aerosol size-dependent below-cloud scavenging by rain and snow in the ECHAM5-HAM, *Atmos. Chem. Phys.*, 9, 4653–4675, doi:10.5194/acp-9-4653-2009, 2009.
- Engelmann, R. J.: Rain scavenging of ZnS particles, *J. Atmos. Sci.*, 22, 719–727, 1965.
- Feng, J.: A 3-mode parameterization of below-cloud scavenging of aerosols for use in atmospheric dispersion models, *Atmos. Environ.*, 41, 6808–6822, 2007.
- Grover, S. N. and Pruppacher, H. R.: The effect of vertical turbulent fluctuations in the atmosphere on the collection of aerosol particles by cloud drops, *J. Atmos. Sci.*, 42, 2305–2318, 1985.
- Hall, W. D.: A detailed microphysical model within a two-dimensional dynamic framework: Model description and preliminary results, *J. Atmos. Sci.*, 37, 2486–2507, 1980.
- Henzing, J. S., Olivié, D. J. L., and van Velthoven, P. F. J.: A parameterization of size resolved below cloud scavenging of aerosols by rain, *Atmos. Chem. Phys.*, 6, 3363–3375, doi:10.5194/acp-6-3363-2006, 2006.
- Jacobson, M. Z.: *Fundamentals of Atmospheric Modeling*, 2nd edition, Cambridge University Press, New York, 813 pp., 2005.
- Khain, A. P. and Pinsky, M. B.: Turbulence effects on the collision kernel, II: Increase of the swept volume of colliding drops, *Q. J. Roy. Meteor. Soc.*, 123, 1543–1560, 1997.
- Laakso, L., Grönholm, T., Rannik, U., Kosmale, M., Fiedler, V., Vehkamäki, H., and Kulmala, M.: Ultrafine particle scavenging coefficients calculated from 6 years field measurements, *Atmos. Environ.*, 37, 3605–3613, 2003.
- Loosmore, G. A. and Cederwall R. T.: Precipitation scavenging of atmospheric aerosols for emergency response applications: testing an updated model with new real-time data, *Atmos. Environ.*, 38, 993–1003, 2004.
- Mircea, M., Stefan, S., and Fuzzi, S.: Precipitation scavenging coefficient: influence of measured aerosol and raindrop size distributions, *Atmos. Environ.*, 34, 5169–5174, 2000.
- Nober, F. J. and Graf, H. F.: A new convective cloud field model based on principles of self-organisation, *Atmos. Chem. Phys.*, 5, 2749–2759, doi:10.5194/acp-5-2749-2005, 2005.
- Park, S. H., Jung, C. H., Jung, K. R., Lee, B. K., and Lee, K. W.: Wet scrubbing of polydisperse aerosols by freely falling droplets, *Aerosol Sci.*, 36, 1444–1458, 2005.
- Seinfeld, J. H. and Pandis, S. N.: *Atmospheric Chemistry And Physics: From Air Pollution To Climate Change*, 1203 pp., Wiley & Sons, New Jersey, 2006.
- Slinn, W. G. N.: Precipitation scavenging, in *Atmospheric Sciences and Power Production –1979*, Chap. 11, Division of Biomedical Environmental Research, US Department of Energy, Washington, DC, 1983.
- Sparmacher, H., Fülber, K., and Bonka, H.: Below-cloud scavenging of aerosol particles: Particle-bound radionuclides – Experimental, *Atmos. Environ.*, 27A, 605–618, 1993.
- Toon, O. B., Turco, R. P., Westphal, D., Malone, R., and Liu M. S.: A multidimensional model for aerosols: Description of computational analogs, *J. Atmos. Sci.*, 45, 2123–2143, 1988.
- Tost, H., Jöckel, P., Kerkweg, A., Sander, R., and Lelieveld, J.: Technical note: A new comprehensive SCAVenging submodel for global atmospheric chemistry modelling, *Atmos. Chem. Phys.*, 6, 565–574, doi:10.5194/acp-6-565-2006, 2006.
- Vohl, O., Mitra, S. K., Wurzler, S., Diehl, K., and Pruppacher, H. R.: Collision efficiencies empirically determined from laboratory investigations of collisional growth of small raindrops in a laminar flow field, *Atmos. Res.*, 85, 120–125, 2007.
- Volken, M. and Schumann, T.: A critical review of below-cloud aerosol scavenging results on Mt. Rigi, *Water Air Soil Poll.*, 68, 15–28, 1993.
- Wang, X., Zhang, L., and Moran, M. D.: Uncertainty assessment of current size-resolved parameterizations for below-cloud particle scavenging by rain, *Atmos. Chem. Phys.*, 10, 5685–5705, doi:10.5194/acp-10-5685-2010, 2010.
- Yum, S. S. and Hudson, G.: Microphysical relationships in warm clouds, *Atmos. Res.*, 57, 81–104, 2001.
- Zhang, L., Michelangeli, D. V., and Taylor P. A.: Numerical studies of aerosol scavenging by low-level, warm stratiform clouds and precipitation, *Atmos. Environ.*, 38, 4653–4665, 2004.